Resistance Spot Welding and Laser Welding Effect on Nickel Tab for Electric Vehicle Battery Development

M Syafiq[1,2,b], N H Jamadon[1,a], A Syahmi[1,c], S Janasekaran[3,d], T Zaharinie[4,e] and R Rangappa[5,f]

[1]Department of Mechanical and Manufacturing Engineering, Faculty of Engineering and Built Environment, Universiti Kebangsaan Malaysia, 43600 Bangi, Selangor, Malaysia
[2]Jabatan Kejuruteraan Mekanikal, Politeknik Banting Selangor, Persiaran Ilmu, Jalan Sultan Abdul Samad, 42700 Banting, Selangor
[3]Center for Advanced Materials and Intelligent Manufacturing, Faculty of Engineering, Built Environment & Information Technology, SEGi University, Petaling Jaya 47810, Selangor
[4]Department of Mechanical Engineering, Faculty of Engineering, University of Malaya, Kuala Lumpur, Malaysia
[5]Department of Mechanical Engineering, BMS Institute of Technology & Management, Bengaluru, Visvesvaraya Technological University, Belagavi, 590018, India

[a)] Corresponding author: nashrahhani@ukm.edu.my
[b)] syafiq.zainun@gmail.com
[c)] syahmisulaimi99@gmail.com
[d)] shaminijanasekaran@segi.edu.my
[e)] tzaharinie@um.edu.my
[f)] ravichandra@bmsit.in

Abstract In this study, the joint ability of two different joining techniques, namely resistance spot welding and laser welding of nickel weld interfaces and joint micro-structure were addressed. Similar materials of nickel joint were used to investigate the parallel connection of tab cells for electric vehicle (EV) battery development. It was found that using the parameters discussed, the joining of two similar nickel were successfully achieved via these welding methods. The results show that the material joints fabricated using laser welding had the highest average stress value of 155.86 MPa, whereas the average for nickel joints of resistance spot welding was 122.25 MPa. In addition, the results of FESEM analysis on the cross-section of the weld material also found that the length of the surface for the material being connected and affects the stress value. For resistance spot welding process, 0.09 s of welding time promoted the formation of sound weld beads with better control of penetration depth and excellent joint interface. Compared to the resistance spot

welding process, laser welding produced a better weld interface, which contributes to a higher strength value.

Keywords Electric vehicle, Joining techniques, Resistance spot welding, Laser welding

1 Introduction

EV batteries consist of battery cells arranged in large numbers in series or parallel. It is important to ensure that optimal power and energy capacity can be supplied to electric vehicles [1]. In addition, vehicle batteries also need to travel through harsh environments. A variety of severe driving conditions such as vibration, bad weather, and humidity, the connections in the battery pack will experience possible mechanical fatigue, high-temperature condition and corrosion [2][3]. The selection of a good joining method is important from the perspective of mechanical strength and microstructure of the welded joint [4].

Connecting battery cells in large quantities is difficult to be implemented due to multi-layers of thin iron which need to be welded together with high conductivity [5]. A very crucial point in an EV is the design and the performance of battery system (traction battery) as part of the electric powertrain [6], [7]. The battery system needs to have both high energy density and power with optimal range and sufficient driving dynamics.

The lithium-ion batteries (Li-ion) were preferred for energy storage due to its characteristic of high-power density. The voltage and current density of a single battery cell will be inadequate for operation in a battery pack. As a result, a battery pack requires the assembly and connection of numerous battery cells, either in series or parallel. The most common way to connect battery cells will be either in series or parallel form, but this is also the main cause of the degradation of consistency between cells [8], [9].

In general, spot welding technique was employed extensively compared with laser welding due to its lower operating cost. However, the quality of the spot welding technique was poorer than the laser welding technique, which it requires some control in several parameter such as the welding force from the electrode welder, electric voltage, electric current, welding time, and electrode geometry as well as the electrode material [10]–[12]. In addition, many battery packs will be manufactured each year for production due to increase in demand. Therefore, batteries must be assembled by using a robust joining process and the development of effective joining technology for battery manufacturing as an important requirement for car manufacturers.

The current research work was focused on the analysis of welded Ni and Ni joints similar materials by using the spot welding process. Three main parameters in spot welding will be used: electrode force, welding current and welding duration. Based

on the findings from literature review, the welding duration parameters will be modified, meanwhile the electrode force and welding current will be maintained throughout the experiment. The effects of different welding parameters such as weld pressure and weld time on the mechanical testing and microstructure of joint area will be studied. In comparison to the laser welding which has very much shorter weld cycle and able to create stronger joints on the basis of the same weld region will be observed.

2 Methodology

This study focuses on laser welding and resistance spot welding against two similar materials, which was the Ni. Resistance and laser welding were employed, as well as assessing the surface of the welding material. The methodology commenced with specimen preparation, continued with the welding procedure, mechanical and microstructural observation, and concluded with the interpretation of the obtained results. Figure 1 exhibits the flow chart of the overall procedure for this experiment. The experimental plan was developed based on the joining requirements for various time of welding parameters.

The specimens to be used were precisely cut into 50 mm x 8 mm dimensions, with the thickness of 0.1 mm, as shown in Figure 1. A 50 mm of nickel was superimposed with a nickel sample of equal size at 10 mm, which portraits in Figure 2. The size of the nickel sample which had been joined was 90 mm after two nickel samples were welded. The sample were analyzed by using Scanning Electron Microscope (SEM) and energy dispersive X-ray (EDX) analysis approach to identify the purity of the specimen used. The resistance spot welding will then be performed using three parameters: welding time, welding current, and electrode force. This experiment will be carried out in three sets, with the only difference being the welding time, which will range between 0.03 s to 0.09 s with a step size of 0.03 s, as given in Table 1.

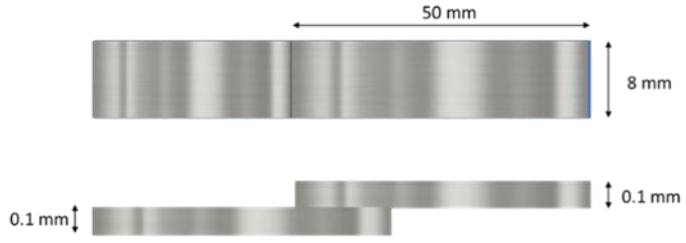

Fig. 1 Ni-Ni welded sample.

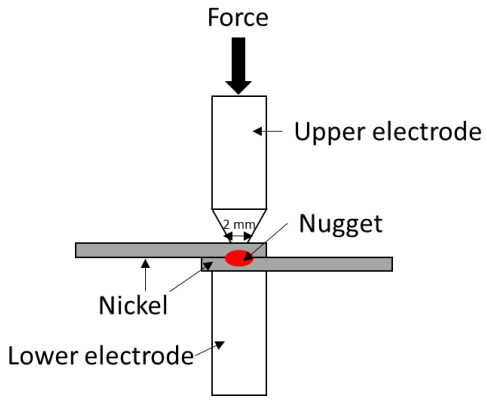

Fig. 2 Schematic of resistance spot welding.

Table 1. Resistance spot welding parameters were used in the study.

Sample	Set 1	Set 2	Set 3
Time	0.03 s	0.06 s	0.09 s
Current		5 kA	
Electrode force		0.3 MPa	
Electrode material		Copper	
Spot welding arrangement		1 spot	

For laser welding, only one parameter was used in this study to compare between the two welding techniques. The parameters used are shown in Table 2. Laser welding is carried out using Ytterbium Fiber Laser Marking Machine.

Table 2. Laser welding parameters were used in the study

Parameter	**Value**
Pulse width	2 ms
Frequency	250 Hz
Power	200 W

Mechanical testing will be performed on the specimen which was completed the spot welding and laser welding processes. Tensile shear tests were carried out on a universal testing equipment in accordance with the ASTM D1002 standard. The tensile shear test was conducted at 0.5 and 1 mm/min. The mechanical performance of the joint results was described by the failure mode. The welded sample will be cut with an EDM wire cutting machine to examine the microstructure, where this sample will then go through with mounting process. The previously analyzed

samples will be ground with a grinding machine. Following that, an optical microscope and field emission scanning electron microscopy (FESEM) will be used to examine the microstructure.

3 Result and Discussions

3.1 Joining samples and optical microscopy of welded surface

Resistance spot welding was used because it is the most suitable method for small scale and limited production. This is because spot welding requires low initial costs and low maintenance costs. It is easy to use and produce good welding quality. Spot welding requires simple setup and can be done semi-automatically or fully automatically. Figure 3 shows spot welding samples with various of timing and laser welded sample. It can be seen that spot welding performed at 0.09 s produces (Figure 3 (c)) highly noticeable weld on the surface of the joint material compared to spot welding at 0.03 s and 0.06 s (Figure 3 (a) and (b), respectively). In addition, the welding results became more significant in parallel with the increase in time. Besides, the sample that was welded using laser welding was observed to result in three layers of circles, as shown in Figure 3 (d). Appearances of laser weld specimen is almost similar with the results obtained by Jian Long et al. [13]. The behavior of laser welded sample will be discussed in detail.

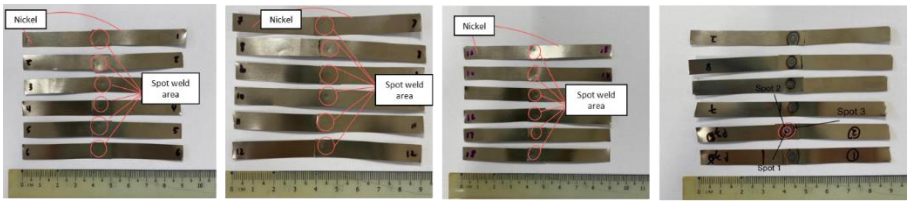

(a) Spot weld 0.03 s (b) Spot weld 0.06 s (c) Spot weld 0.09 s (d) Laser weld 2 ms

Fig. 3 Ni-Ni welded samples at various weld times of (a) 0.03, (b) 0.06 s, (c) 0.09 s, and (d) laser welded sample.

Microscope images of welded specimens are shown in Figure 4. The figures 4 (a)-(c) shows microscope images of resistance spot welding samples with welded time of 0.03 s, 0.06 s and 0.09 s, respectively. It was found that the size of the resulting weld on the nickel surface was the same as the size of the copper electrode used (2 mm). In addition, the welding results shows it became more significant in parallel with the increase in time. This is because spot welding performed at 0.09 s produces a more noticeable weld on the surface of the joint material compared to spot welding at 0.03 s and 0.06 s.

Laser welding was used to join nickel sheets because it is a non-contact process, which can produce high precision welds and has shorter cycle time. The orientation of the nickel sheet during laser welding was the same as in resistance spot welding. It was found that the sample welded using laser welding has three layers of circles as resulted in Figure 3 (d). Spot 1 is the part of the joint which was exposed to the laser light directly, while spot 2 is the part of the heat affected zone (HAZ). Next, spot 3 is the part resulting from oxidation on the outside of the connection. This may occur due to the reaction that occurs between the laser and oxygen as it was performed in normal atmosphere conditions [11]. In contrast, laser welding produces three spots on the surface of the joint, with spot 1 having the same size as the groove's radius (beam radius) created during welding

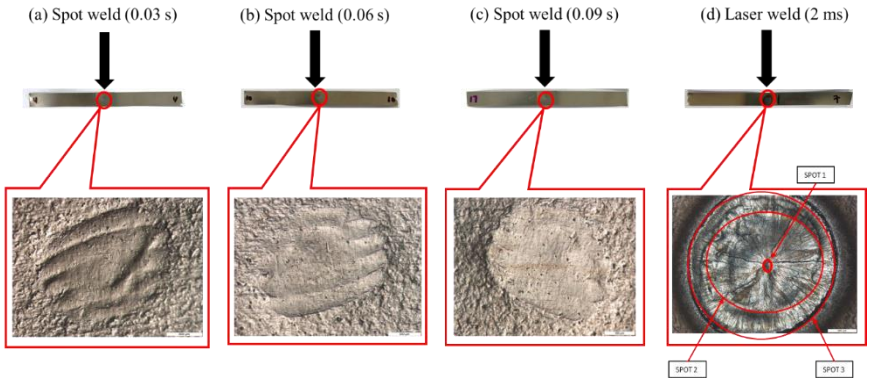

Fig. 4 Surface microstructure of the joining parts.

3.2 Joint Strength

Figure 5 exhibits the shear test of the joint strength for spot welding and laser welding. From the shear test result, the highest stress strength resulted in spot welding at the 0.09 s parameter which was 132.83 MPa while the minimum stress resulted in spot welding using the 0.03 s parameter at 125.48 MPa. Whereas the joint strength of spot welding sample welded at 0.06 s was 127.37 MPa. The results show that increasing of welding time will eventually rises the heat generated in the welding zone and causes the weld area to expand, resulting in an increase in joint strength. As such, more in-depth testing can be done using different parameters.

Shear tests were also performed on welded joints using laser welding. The average stress value resulting from laser welding was 155.86 MPa. It was found that laser welding can produce a stronger Ni - Ni connection than resistance spot welding at parameters as due to the optimal welding geometry that can be achieved and has a high-power density. The heat source produced by the laser beam was highly

concentrated. This is in line with the study by Das et al. [14] which states that various types of metals and conductors with thickness of several millimeters can be welded due to the high-power density of the laser beam. Hence, it may be assumed that a smaller spot makes it possible to weld with less power, minimizing the amount of heat produced by the process. Additionally, faster welding speeds can be used, which makes production more efficient and enhanced the joint reliability.

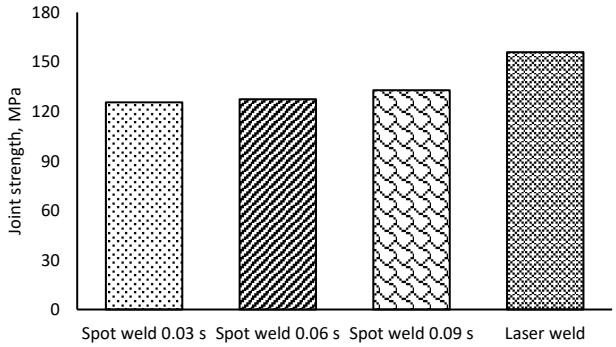

Fig. 5 Shear strength of weld sample.

3.3 Fracture surface morphology

The morphology of fracture surface conditions were seen in Figure 6. According to the shear test findings, all of the samples for spot welding, Figure 6 (a)-(c) had tearing failure on the base material, which is on the Ni section, but no failure on the welding joint part. This occurs because the strength of the resulting weld joint is greater than the strength of the material. It may be presumed that all of the samples welded using both techniques were completely joined at the spot weld area. There are several possibilities for failure. An adhesive failure happens when the bond between the adhesive layer and one of the adhesives fails. Joint failure frequently comprises many failure mechanisms and was measured as a proportion of adhesive failure. From this study, it can be assumed that the tearing that occurs in the base material for resistance spot welding may be caused by the orientation of the sample during the tension test, as depicted in Figure 7, which permits tearing to occur despite the lower stress value produced on the resistance spot welding joint sample.

In laser welding, however, the connection is not severed at base material, but rather at spots 1, 2 and 3, as shown in Figure 6 (d). This could be the result of the Ni undergoing metallurgical fusion. It was also discovered that the laser weld has a heat-affected zone (HAZ), which increases the joint area and thus influences the joint ability. It was revealed that fracture occurred in the fused zone on the laser weld region when welding occurred in a larger spot. This result is comparable to

that of a previous study by Dimatteo et al. [15].This demonstrates that the link between the size of the welded surface and the measured stress value was directly proportional.

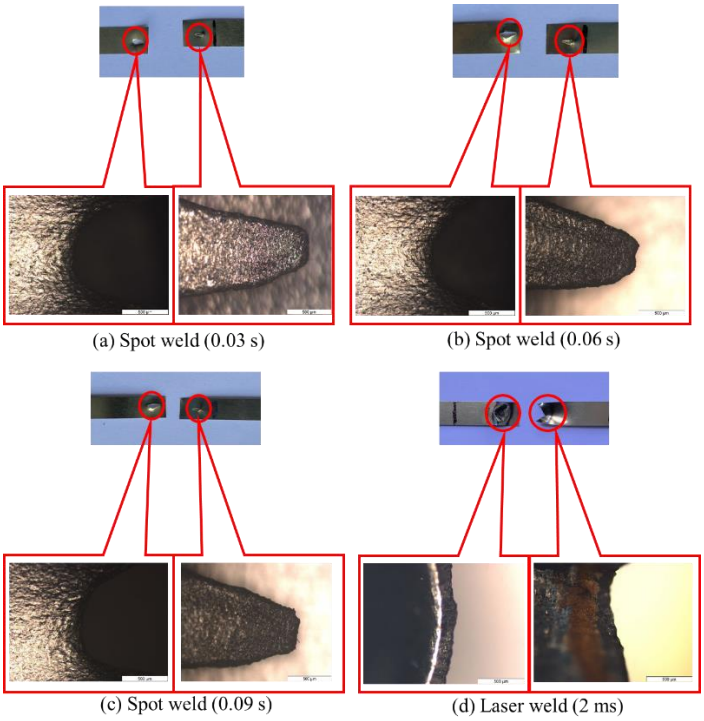

Fig. 6 Morphology of fractured surfaces of Ni-Ni samples (a) spot weld at 0.03 s, (b) spot weld at 0.06 s, (c) spot weld at 0.09 s, and (d) laser weld 2 ms.

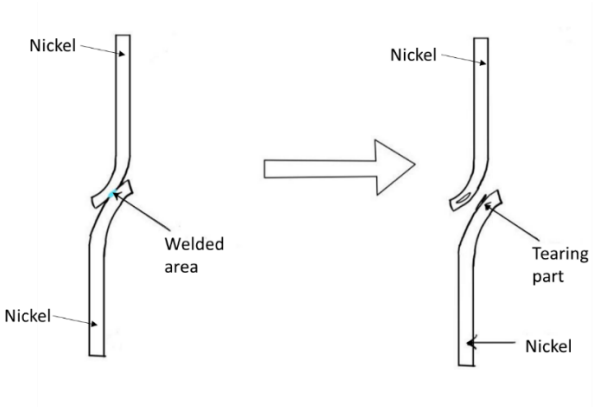

4 Conclusion

Based on the results obtained, it was found that the joining of Ni materials using laser welding has the highest average stress value of 155.86 MPa while the average for connection of materials using resistance spot welding was 122.25 MPa. In addition, for the joining of materials using resistance spot welding, three parameters have been used which were at 0.03 s, 0.06 s, and 0.09 s, and based on the data obtained the joining of materials using resistance spot welding at 0.09 s was able to produce higher stress values compared to the other parameter at 132.83 MPa. From the observation through optical microscope, it was found that tearing has occurred on all resistance spot welding material samples. The laser weld joining occurs in the heat-affected zone (HAZ), where Ni undergoes metallurgical fusion, contributing to the greatest joint strength value of 155.86 MPa. Based on observations, it was found that both types of welding were successful in joining two similar Ni materials using the parameters that have been discussed.

Acknowledgements

The authors gratefully acknowledge the financial support by the Universiti Kebangsaan Malaysia (GGPM-2019-064). Special thanks to the contributors from University of Malaya, Segi University, and BMS Institute of Technology and Management, India for this project.

References

1. W. Dang, L. Manjakkal, W. T. Navaraj, L. Lorenzelli, V. Vinciguerra, and R. Dahiya, “Stretchable wireless system for sweat pH monitoring,” Biosens. Bioelectron., vol. 107, pp. 192–202, 2018, doi: 10.1016/j.bios.2018.02.025.
2. T. Chang et al., “A General Strategy for Stretchable Microwave Antenna Systems using Serpentine Mesh Layouts,” Adv. Funct. Mater., vol. 27, no. 46, 2017, doi: 10.1002/adfm.201703059.
3. C. G. Núñez, W. T. Navaraj, E. O. Polat, and R. Dahiya, “Energy-Autonomous, Flexible, and Transparent Tactile Skin,” Adv. Funct. Mater., vol. 27, no. 18, 2017, doi: 10.1002/adfm.201606287.
4. B. You, Y. Kim, B. K. Ju, and J. W. Kim, “Highly Stretchable and Waterproof Electroluminescence Device Based on Superstable Stretchable Transparent Electrode,” ACS Appl. Mater. Interfaces, vol. 9, no. 6, pp. 5486–5494, 2017, doi: 10.1021/acsami.6b14535.

5. S. Zulfiqar, A. A. Saad, M. W. Chek, M. F. M. Sharif, Z. Samsudin, and M. Y. T. Ali, “Structural and Random Vibration Analysis of LEDs Conductive Polymer Interconnections,” IOP Conf. Ser. Mater. Sci. Eng., vol. 815, no. 1, 2020, doi: 10.1088/1757-899X/815/1/012003.
6. S. Zulfiqar et al., “Alternative manufacturing process of 3-dimensional interconnect device using thermoforming process,” Microelectron. Reliab., vol. 127, p. 114373, 2021, doi: https://doi.org/10.1016/j.microrel.2021.114373.
7. S. Zulfiqar, A. A. Saad, Z. Ahmad, F. Yusof, and Z. Bachok, “Structural Analysis and Material Characterization of Silver Conductive Ink for Stretchable Electronics,” Int. J. Integr. Eng., vol. 13, no. 7, pp. 128–135, 2021, [Online]. Available: https://publisher.uthm.edu.my/ojs/index.php/ijie/article/view/9536.
8. N. A. Aziz, A. A. Saad, Z. Ahmad, S. Zulfiqar, F. C. Ani, and Z. Samsudin, “Chapter 8 - Stress analysis of stretchable conductive polymer for electronics circuit application,” in Handbook of Materials Failure Analysis, A. S. H. Makhlouf and M. Aliofkhazraei, Eds. Butterworth-Heinemann, 2020, pp. 205–224.
9. S. Zulfiqar, A. A. Saad, Z. Ahmad, F. Yusof, and K. Fakpan, “Analysis And Characterization Of Polydimethylsiloxane (Pdms) Substrate By Using Uniaxial Tensile Test And Mooney-Rivlin Hyperelastic MODEL,” J. Adv. Manuf. Technol., vol. 16, no. 1, 2022, [Online]. Available: https://jamt.utem.edu.my/jamt/article/view/6280.
10. K. K. Chawla, Composite Materials: Science and Engineering. Springer International Publishing, 2019.
11. Y. Liu and F. Dai, “A review of experimental and theoretical research on the deformation and failure behavior of rocks subjected to cyclic loading,” J. Rock Mech. Geotech. Eng., vol. 13, no. 5, pp. 1203–1230, 2021, doi: 10.1016/j.jrmge.2021.03.012.
12. W. Grellmann and S. Seidler, Polymer Testing. Hanser Munich, 2013.
13. A. Głuchowski and W. Sas, “Long-term cyclic loading impact on the creep deformation mechanism in cohesive materials,” Materials (Basel)., vol. 13, no. 17, 2020, doi: 10.3390/ma13173907.
14. J. Beter et al., “Viscoelastic behavior of glass-fiber-reinforced silicone composites exposed to cyclic loading,” Polymers (Basel)., vol. 12, no. 9, p. 1862, Aug. 2020, doi: 10.3390/POLYM12091862.
15. E. Bociaga, M. Kula, and K. Kwiatkowski, “Analysis of structural changes in injection-molded parts due to cyclic loading,” Adv. Polym. Technol., vol. 37, no. 6, pp. 2134–2141, 2018, doi: 10.1002/adv.21872.
16. K. Yu, H. Li, A. J. W. McClung, G. P. Tandon, J. W. Baur, and H. J. Qi, “Cyclic behaviors of amorphous shape memory polymers,” Soft Matter, vol. 12, no. 13, pp. 3234–3245, 2016, doi: 10.1039/c5sm02781k.
17. N. Rozo Lopez, J. Chen, and C. Hopmann, “A micromechanical model for loading and unloading behavior of fiber reinforced plastics under cyclic loading,” Polym. Compos., vol. 41, no. 9, pp. 3892–3902, 2020, doi: 10.1002/pc.25684.
18. M. Ly, K. A. Khan, and A. Muliana, “Modeling Self-heating under Cyclic Loading in Fiber-Reinforced Polymer Composites,” J. Mater. Eng. Perform., vol. 29, no. 2, pp. 1321–1335, 2020, doi: 10.1007/s11665-020-04663-7.
19. X. Zheng, Q. Wang, J. Luan, Y. Li, and N. Wang, “Patterned Metal/Polymer Composite Film with Good Mechanical Stability and Repeatability for Flexible Electronic Devices

Using Nanoimprint Technology.," Micromachines, vol. 10, no. 10, Sep. 2019, doi: 10.3390/mi10100651.

20. M. Miraftab, Fatigue failure of textile fibres. Elsevier Science, 2009.
21. S. K. Paul, "A critical review of experimental aspects in ratcheting fatigue: microstructure to specimen to component," J. Mater. Res. Technol., vol. 8, no. 5, pp. 4894–4914, 2019, doi: 10.1016/j.jmrt.2019.06.014.